

Boston, July-August 1969 (Massachusetts Institute of Technology, Cambridge, Mass., 1969), p. 862

⁷D. H. Jaecks, B. Van Zyl, and R. Geballe, Phys. Rev. **137**, A340 (1965).

⁸E. P. Andreev, A. Ankudinov, and S. V. Bobashev, Zh. Eksp. Teor. Fiz. **50**, 565 (1966) [Sov. Phys.-JETP

23, 375 (1966)].

⁹H. H. Michels, J. Chem. Phys. **44**, 3834 (1966).

¹⁰M. R. Flannery, J. Phys. B: Proc. Phys. Soc., London **3**, 306 (1970).

¹¹I. M. Cheshire, J. Phys. B: Proc. Phys. Soc., London **1**, 428 (1968).

VACUUM-ULTRAVIOLET LASER ACTION OBSERVED IN THE LYMAN BANDS OF MOLECULAR HYDROGEN

R. T. Hodgson

IBM Thomas J. Watson Research Center, Yorktown Heights, New York 10598

(Received 5 June 1970)

Stimulated emission has been observed in the *P*-branch lines of the 3-10, 4-11, 5-12, 6-13, and 7-13 Lyman bands ($v' - v''$, $B^1\Sigma_u^+ \rightarrow X^1\Sigma_g^+$) of molecular hydrogen near 1600 Å. Light pulses of approximately 2 nsec duration and 1.5 kW maximum power were produced using a Blumlein parallel-plate transmission line discharging through hydrogen gas at pressures between 20 and 150 Torr.

The first observation of stimulated emission in the vacuum-ultraviolet spectral range is reported in this Letter. The wavelengths of the laser light near 1600 Å are the shortest wavelengths achieved to this time, and the pulse power and energies available should make this type of laser useful for studying the interaction of high-energy photons with matter.

The lasing action is produced by inverting the population of an excited electronic state of a diatomic molecule with respect to the high vibrational-rotational levels of the ground state. This general scheme was in fact proposed by Bazhulin, Knyazev, and Petrash¹ in 1965. Figure 1 shows an energy-level diagram of the hydrogen molecule. A fast electrical discharge in hydrogen gas was used to excite the $B^1\Sigma_u^+$ vibrational-rotational levels. The dashed vertical lines represent the electron-collision-induced transitions between the zeroth vibrational level of the $X^1\Sigma_g^+$ ground state and the v' levels of the upper states. Since the high-energy electron collisions populate the electronic states much more efficiently than the upper vibrational levels of the ground state, inversion densities and gain were high enough to produce stimulated emission without mirrors in *P*-branch lines of the 3-10, 4-11, 5-12, 6-13, and 7-13 Lyman bands ($B^1\Sigma_u^+ \rightarrow X^1\Sigma_g^+$). These transitions are indicated by the solid vertical lines in Fig. 1.

In order to generate the high-power fast-pulsed electrical discharge needed to produce a large inversion and high gain at vacuum-ultraviolet wavelengths, a Blumlein circuit parallel-plate

strip line and discharge channel similar to that described by Shipman² was constructed. Figure

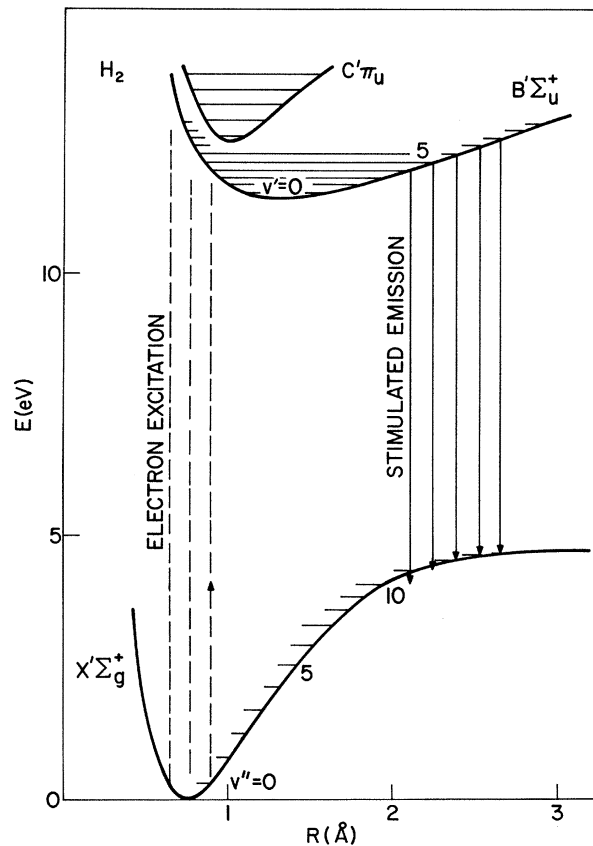


FIG. 1. Potential energy curves for the $X^1\Sigma_g^+$, $B^1\Sigma_u^+$, and $C^1\Pi_u$ states of the hydrogen molecule. The potential energy in electron volts is plotted as a function of internuclear distance in Å.

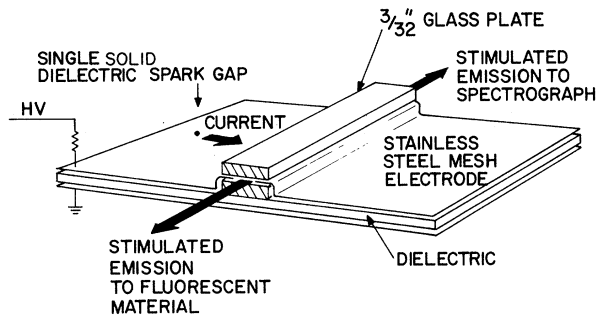


FIG. 2. Blumlein circuit flat-plate transmission line and discharge-tube arrangement. Electrode dimensions are $40 \times 80 \text{ cm}^2$. 0.040-cm Mylar was used as the dielectric to hold off 30 kV dc. Torr-seal epoxy was used to cement the 23-cm mesh between the two glass plates forming the sides of the discharge channel.

2 shows the experimental arrangement. The discharge was contained in a $120 \times 1.2 \times 0.04 \text{ cm}^3$ channel made by sandwiching the high-voltage current-carrying electrodes between two long thin glass plates. Stainless-steel mesh was used for these electrodes so that the cut edges would provide lines of sharp metal points in the gas to make the breakdown and discharge more uniform.³ A single mechanically ruptured solid dielectric switch was used to initiate the discharge.

Figure 3(a) shows a spectrum of the laser emission taken in the first order using a McPherson model 225 1-m normal-incidence vacuum monochromator equipped with a film holder and a 1200-line/mm grating. Wavelengths were measured absolutely to within 1 \AA using a zero-order mark and the monochromator setting. Relative wavelengths agreed to within the 0.05-\AA measuring error with Herzberg and Howe's⁴ measured wavelengths for the assigned lines.

The stimulated emission spectrum shown in Fig. 3(a) and the microdensitometer trace shown in Fig. 3(b) can be explained using Spindler's⁵ published Franck-Condon factors for the molecular hydrogen Lyman band intensities in conjunction with the intensity and selection rules for $J' \rightarrow J''$ transitions within each band.⁶

The probability of exciting a hydrogen molecule in the $v''=0$ level of the $X^1\Sigma_g^+$ ground state to a given vibrational level v' of the $B^1\Sigma_u^+$ state is proportional to the $v'-0$ Franck-Condon factors. These factors increase⁵ with v' until they reach 0.074 at $v'=7$. For each v' , the probability of exciting the various rotational levels can be predicted since excitations of odd-to-odd rotational levels are forbidden by symmetry.⁶ Thus, since two-thirds of the hydrogen molecules are in the

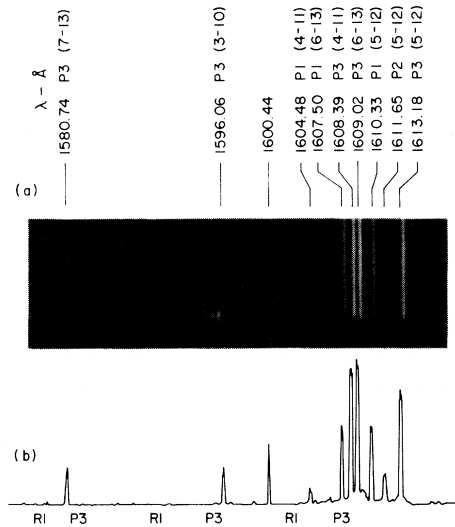


FIG. 3. (a) Stimulated emission spectra showing some of the P -branch lines of the 3-10, 4-11, 5-12, 6-13, and 7-13 Lyman bands ($B^1\Sigma_u^+ \rightarrow X^1\Sigma_g^+$) of molecular hydrogen. (b) Microdensitometer trace of this spectrum. Some of the missing $R(1)$ line positions are also noted along with their corresponding $P(3)$ lines.

$X^1\Sigma_g^+$, $v''=0, J''=1$ orthohydrogen state⁶ in equilibrium at room temperature, we would expect most electron collisions to populate the $v', J'=2$, and $J'=0$ levels of the higher-energy electronic states. If the electron-collision transition probabilities are determined by the same statistical weight arguments as the optical transition probabilities, the ratio⁶ would in fact be 2:1. Now, the $J'=2$ levels can only radiate to the $J''=3$ or the $J''=1$ levels of the various ground electronic vibrational states [the $P(3)$ and $R(1)$ lines of the bands]. The branching ratio⁶ for emission from these lines is determined by the statistical weights of the rotational levels and is numerically equal to 1.5:1 for the $P(3)$ and $R(1)$ lines. In fact, only a single $P(3)$ line from each $J'=2$ level is seen, and that line belongs to the band with the largest Franck-Condon factor. This perturbation of emission intensities from that seen in spontaneous emission proves that the $J'=2$ states have been stimulated to emit in the $P(3)$ lines. With highest discharge powers, sufficient population builds up in the $J'=0$ level of the $v'=5$ and 6 vibrational states and the $J'=1, v'=5$ level that emission is stimulated in the $P(1)$ lines of the 5-12 and 6-13 bands, and in the $P(2)$ line of the 5-12 band.

Estimates of laser energy, pulse length, and power were made by converting the ultraviolet pulses to visible radiation using fluorescent scintillators coated on the inside of the discharge

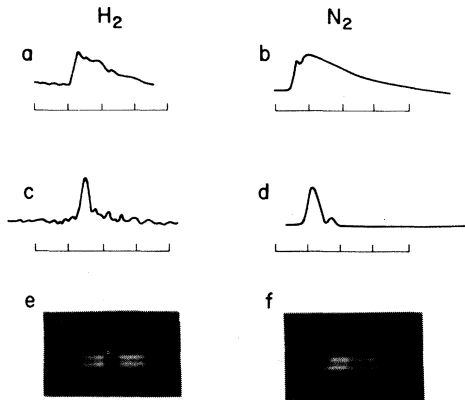


FIG. 4. (a) Fluorescence intensity of sodium salicylate coated on the inside of the discharge tube window when excited by a hydrogen laser pulse at $\sim 1600 \text{ \AA}$. (b) Fluorescence intensity of the sodium salicylate coating when excited by a nitrogen laser pulse at 3371 \AA . (c) Fluorescence intensity of BBO excited by a hydrogen laser pulse. (d) Intensity of N_2 laser pulse measured directly as a function of time with no fluorescent window in place. The measuring apparatus rise-time is less than $\frac{1}{2}$ nsec. (e) Fluorescence pattern observed with H_2 laser pulse. (f) Fluorescence pattern observed with N_2 laser pulse. The 3371-\AA light can pass through a gap in the scintillator coated on the inside of the window, through the Pyrex, and excite the scintillator coated on the outside. Horizontal scale: $1 \text{ div} = 5 \text{ nsec}$.

tube window. Figures 4(a) and 4(b) can be used to compare the response of sodium salicylate excited by the $\sim 1600\text{-\AA}$ light pulse [4(a)] with that excited by a 3371-\AA light pulse from a molecular nitrogen laser [4(b)]. A trace of the intensity of fluorescence excited in BBO (2, 5-dibiphenyloxazole) reproduced in Fig. 4(c) shows the hydrogen laser pulse shape more clearly than the sodium salicylate because its fluorescence lifetime is of the order of 1 nsec.⁷ The nitrogen laser pulse height and width were directly measured with a biplanar photodiode, and intensity-versus-time traces such as that given in Fig. 4(d) were used to calibrate the response of the sodium salicylate to fast light pulses of 3371-\AA wavelength. Since the quantum efficiency of the scintillator is constant⁸ between 400 and 3400 \AA , the total energy contained in the hydrogen laser pulse could be estimated to be about $3 \mu\text{J}$.

The pulse energies plotted as a function of hydrogen pressure showed a broad maximum near 60 Torr. At about 20 and 150 Torr, the fluorescent intensity dropped below the detection level of our TRG 105B, S-20 response, biplanar photodiode, and Tektronix 119 oscilloscope combina-

tion.

The pulse length was estimated to be ~ 2 nsec by measuring the risetime of the sodium salicylate fluorescence. These estimated values of energy and pulse length correspond to a power of 1.5 kW.

Photographs of the fluorescent patterns of the two laser beams are given in Figs. 4(e) and 4(f). They appear similar except that the 3371-\AA laser light can pass through a gap left in the inside fluorescent coating, through the Pyrex window, and excite a fluorescent strip coated on the outside of the window in a position complementary to the gap in the inside coating.

Stimulated emission was proposed initially by Bazhulin, Knyazev, and Petrash¹ on the $C^1\Pi_u \rightarrow X^1\Sigma_g^+$ Werner band transitions in hydrogen in the 1100-\AA region. They pointed out that a diatomic molecular system with the minimum of the ground-state- and excited-state-potential curves at different internuclear distances implied large probabilities of emission to high vibrational levels. Ali and Kolb⁹ simulated the discharge parameters of Shipman's² device with a computer, and predicted lasing action on the Werner bands in the region $1025\text{-}1239 \text{ \AA}$. They did not treat the excitation of the $B^1\Sigma_u^+$ in detail. In fact, the Franck-Condon factors for the Lyman bands are lower than for the Werner bands. In the discharge, however, more electrons have sufficient energy to excite the $B^1\Sigma_u^+$, $v' = 1\text{-}7$ vibrational levels than the $C^1\Pi_u$ state since the threshold energies are smaller. This would explain the fact that no stimulated emission on the Werner bands is seen, and that the power output in the $v' = 7$ band is less than the $v' = 5$ band.

Stimulating discussions with P. P. Sorokin and J. A. Armstrong, and the technical assistance of S. Baliozian are gratefully acknowledged.

¹P. A. Bazhulin, I. N. Knyazev, and G. G. Petrash, *Zh. Eksp. Teor. Fiz.* **48**, 975 (1965) [*Sov. Phys.-JETP* **21**, 649 (1965)].

²J. D. Shipman, Jr., *Appl. Phys. Lett.* **10**, 3 (1967).

³H. W. Furamoto and H. L. Ceccon, *Appl. Opt.* **8**, 1613 (1969).

⁴G. Herzberg and L. L. Howe, *Can. J. Phys.* **37**, 636 (1959).

⁵R. J. Spindler, AVSSD 0287-66-RR, NASA Report No. CR 72107.

⁶G. Herzberg, *Molecular Spectra and Molecular Structure: I. Spectra of Diatomic Molecules* (Van Nostrand, Princeton, N. J., 1950).

⁷I. B. Berlman, *Handbook of Fluorescence Spectra of Aromatic Molecules* (Academic, New York, 1965).

⁸J. A. R. Samson, *Techniques of Vacuum Ultraviolet Spectroscopy* (Wiley, New York, 1967).

⁹A. W. Ali and A. C. Kolb, *Appl. Phys. Lett.* **13**, 259 (1968).

¹⁰H. S. W. Massey, *Electronic and Ionic Impact Phenomena* (Clarendon, Oxford, England, 1969).

MEASUREMENT OF SPECTRUM OF TURBULENCE WITHIN A COLLISIONLESS SHOCK BY COLLECTIVE SCATTERING OF LIGHT

C. C. Daughney, L. S. Holmes, J. W. M. Paul

United Kingdom Atomic Energy Authority, Research Group, Culham Laboratory, Abingdon, Berkshire, England
(Received 3 April 1970; revised manuscript received 31 July 1970)

We present experimental evidence for the presence of current-driven ion-wave turbulence within a collisionless shock. The frequency and wave-number spectra of this turbulence have been measured by scattering light from the shock front. These measurements are compared with the assumptions and predictions of nonlinear theory.

Shock experiment.—We are studying¹⁻³ a collisionless shock with low Alfvén Mach number ($M_A < 3$), which propagates perpendicular to a magnetic field. The shock is produced by the radial compression of an initial hydrogen plasma by a linear z pinch. The initial plasma conditions ($n_{e1} = 6.4 \times 10^{20} \text{ m}^{-3}$, $T_{i1} = T_{e1} = 1.2 \text{ eV}$, $B_{z1} = 0.12 \text{ T}$) and the shock parameters ($M_A = 2.5$, $V_s = 240 \text{ km sec}^{-1}$, $L_s = 1.4 \text{ mm}$) have been described previously. The electron heating within the shock ($T_{e2} = 44 \text{ eV}$) implies a resistivity which is two orders of magnitude larger than the Spitzer value; the corresponding effective electron collision frequency $\nu^* \sim 3 \text{ GHz}$.

The compression of the magnetic field in the shock front gives rise to an azimuthal current with an electron drift velocity $V_D > C_s$, the ion-sound speed. Linear stability theory⁴⁻⁶ predicts current-driven ion-wave instability, while nonlinear theory⁷ predicts ion-wave turbulence.

Scattering experiments.—We have previously^{2,3} measured a suprathermal level of ion-wave fluctuations within the shock front. The measured level, about 400 times thermal, agrees with that required by a stochastic model of the electron heating.

We now report measurements of the wave-number (k) spectrum and the frequency (ω) spectrum of these ion-wave fluctuations, using essentially the same technique of scattering ruby-laser light.^{3,8-10} This yields the Fourier transform of the electron density fluctuations in the form $S(\omega, \vec{k}) \propto \langle \delta n_e^2(\omega, \vec{k}) \rangle$, with $S(\vec{k}) = \int S(\omega, \vec{k}) d\omega$ and $S_k(\omega) = S(\omega, \vec{k})$ for constant \vec{k} .

In the experiments light is scattered from a 50-mW ruby-laser beam during the transit of the shock through the beam. The pulse of scattered

light is detected by a photomultiplier, either directly or after spectral resolution. The geometry of the incident- and scattered-light paths defines a mean wave vector \vec{k}_m , with $|k_m| \sim 1/\lambda_{Dm}$ (λ_{Dm} is Debye length for mean shock conditions) and with \vec{k}_m in the (r, θ) plane at an angle φ to the azimuthal electron current in the shock front.

Spectrum $S(\vec{k})$.—The observations are made through a window which is covered by different masks in order to vary either the scattering angle within the range $3.3^\circ < \theta < 6.9^\circ$ and hence $|k|$, or the scattering plane within the range $-16^\circ < \varphi < +16^\circ$. Over this range of φ the scattered signal is independent of φ to an accuracy of $\pm 15\%$.¹¹ The dependence of $S(\vec{k})$ on $|\vec{k}|$ is shown in Fig. 1;

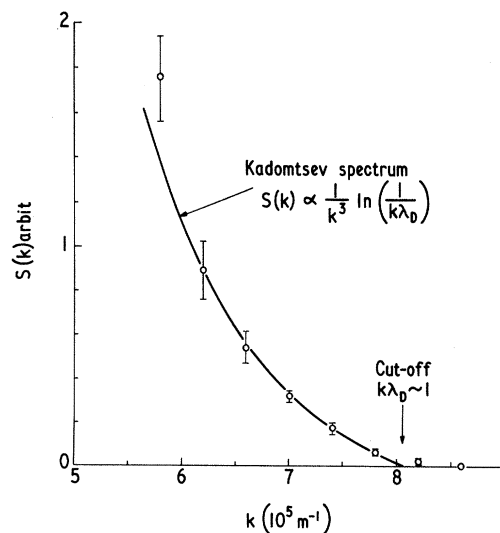


FIG. 1. Wave number spectrum $S(k)$: Experimental points are mean of five measurements and error bars are standard deviation of the mean. The curve is a Kadomtsev spectrum.

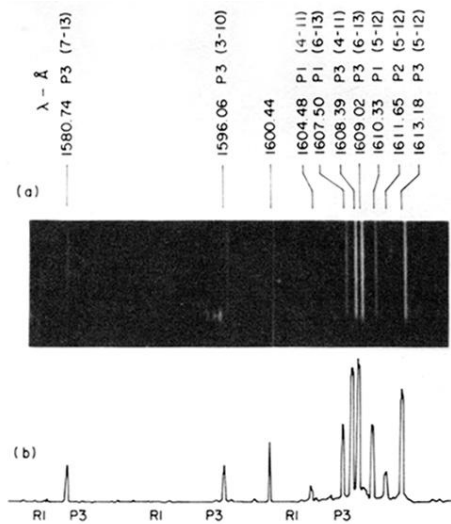


FIG. 3. (a) Stimulated emission spectra showing some of the *P*-branch lines of the 3-10, 4-11, 5-12, 6-13, and 7-13 Lyman bands ($B^1\Sigma_u^+ \rightarrow X^1\Sigma_g^+$) of molecular hydrogen. (b) Microdensitometer trace of this spectrum. Some of the missing *R*(1) line positions are also noted along with their corresponding *P*(3) lines.

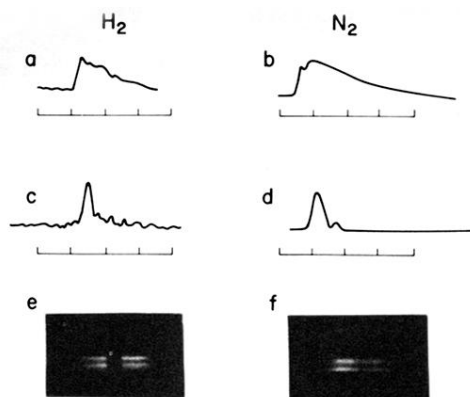


FIG. 4. (a) Fluorescence intensity of sodium salicylate coated on the inside of the discharge tube window when excited by a hydrogen laser pulse at $\sim 1600 \text{ \AA}$. (b) Fluorescence intensity of the sodium salicylate coating when excited by a nitrogen laser pulse at 3371 \AA . (c) Fluorescence intensity of BBO excited by a hydrogen laser pulse. (d) Intensity of N_2 laser pulse measured directly as a function of time with no fluorescent window in place. The measuring apparatus rise-time is less than $\frac{1}{2}$ nsec. (e) Fluorescence pattern observed with H_2 laser pulse. (f) Fluorescence pattern observed with N_2 laser pulse. The 3371-\AA light can pass through a gap in the scintillator coated on the inside of the window, through the Pyrex, and excite the scintillator coated on the outside. Horizontal scale: 1 div = 5 nsec.